
This item was submitted to [Loughborough's Research Repository](#) by the author.
Items in Figshare are protected by copyright, with all rights reserved, unless otherwise indicated.

Evaluation of fracture toughness of ZrO₂ and Si₃N₄ engineering ceramics following CO₂ and fibre laser surface treatment

PLEASE CITE THE PUBLISHED VERSION

<http://dx.doi.org/10.1016/j.optlaseng.2010.09.010>

PUBLISHER

© Elsevier

VERSION

AM (Accepted Manuscript)

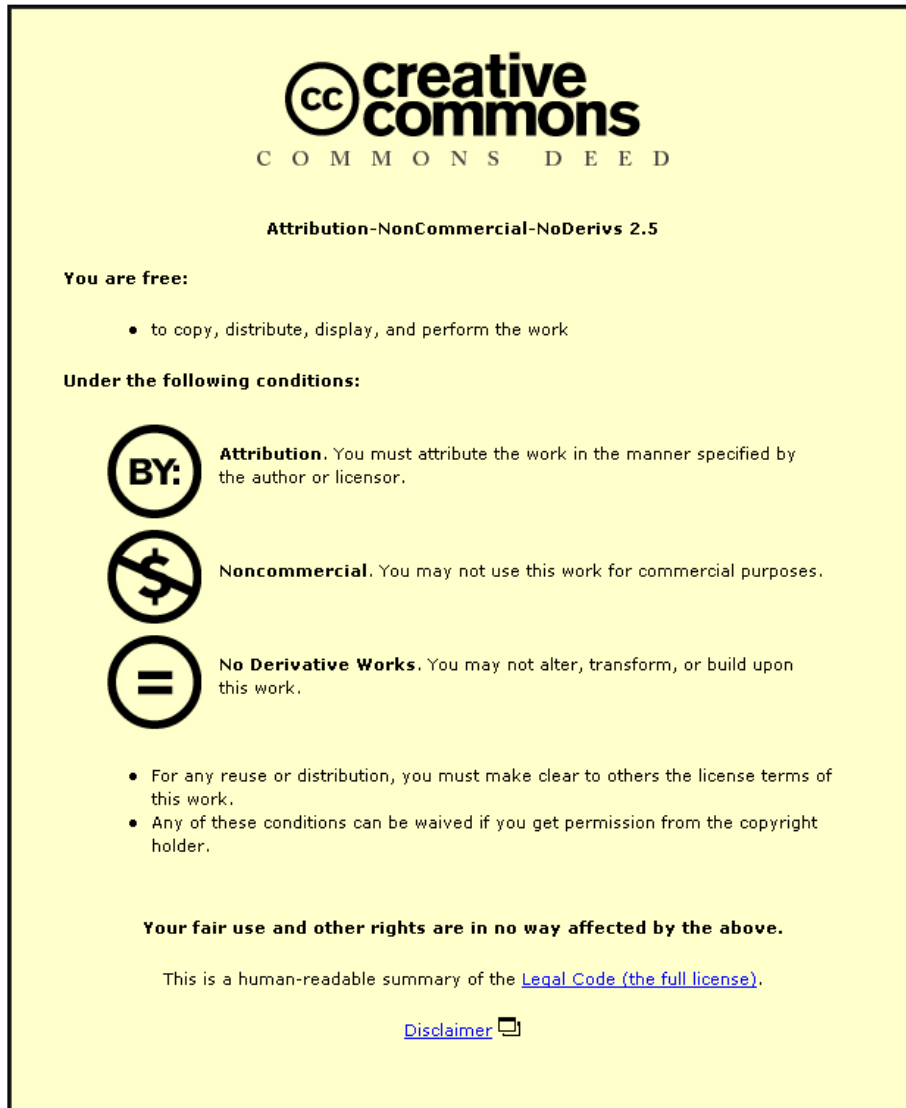
LICENCE

CC BY-NC-ND 4.0

REPOSITORY RECORD

Shukla, Pratik P., and Jonathan Lawrence. 2019. "Evaluation of Fracture Toughness of Zro2 and Si3n4 Engineering Ceramics Following CO2 and Fibre Laser Surface Treatment". figshare. <https://hdl.handle.net/2134/7803>.

This item was submitted to Loughborough's Institutional Repository (<https://dspace.lboro.ac.uk/>) by the author and is made available under the following Creative Commons Licence conditions.



CC creative commons
COMMONS DEED

Attribution-NonCommercial-NoDerivs 2.5

You are free:

- to copy, distribute, display, and perform the work

Under the following conditions:

BY: **Attribution.** You must attribute the work in the manner specified by the author or licensor.

Noncommercial. You may not use this work for commercial purposes.

No Derivative Works. You may not alter, transform, or build upon this work.

- For any reuse or distribution, you must make clear to others the license terms of this work.
- Any of these conditions can be waived if you get permission from the copyright holder.

Your fair use and other rights are in no way affected by the above.

This is a human-readable summary of the [Legal Code \(the full license\)](#).

[Disclaimer](#) 

For the full text of this licence, please go to:
<http://creativecommons.org/licenses/by-nc-nd/2.5/>

Evaluation of Fracture Toughness of ZrO₂ and Si₃N₄ Engineering Ceramics Following CO₂ and Fibre Laser Surface Treatment

P. P. Shukla* and J. Lawrence ^Ψ

Corresponding Author's Details:

Pratik P. Shukla*,
Loughborough University,
Wolfson School of Mechanical and Manufacturing Engineering,
Leicestershire,
LE11 3TU,
United Kingdom,
Email: P.Shukla@lboro.ac.uk,
Direct Line: +44 (0) 1509227592

Second Author's Details:

Jonathan Lawrence ^Ψ
Lincoln School of Engineering,
University of Lincoln,
Brayford Pool,
Lincoln,
LN6 7TS,
United Kingdom

Abstract

The fracture toughness property (K_{1C}) of Si_3N_4 and ZrO_2 engineering ceramics was investigated by means of CO_2 and a fibre laser surface treatment. Near surface modifications in the hardness was investigated by employing the Vickers indentation method. Crack lengths and geometry were then measured by using the optical. A co-ordinate measuring machine was used to investigate the diamond indentations and to measure the lengths of the cracks. Thereafter, computational and analytical methods were employed to determine the K_{1C} . An increase in the K_{1C} of both ceramics was found by the CO_2 and the fibre laser surface treatment in comparison to the as-received surfaces. The K_{1C} of the CO_2 laser radiated surface of the Si_3N_4 was over 3 % higher in comparison to that of the fibre laser treated surface. This was by softening of the near surface layer of the Si_3N_4 which comprised of lower in hardness, which in turn increased the crack resistance. The effects were not similar with the ZrO_2 ceramic to that of the Si_3N_4 as the fibre laser radiation in this case had produced a rise of 34% compared to that of the CO_2 laser radiation. This occurred due to propagation of lower crack resulting from the Vickers indentation test during the fibre laser surface treatment which inherently affected the end K_{1C} though an induced compressive stress layer. The K_{1C} modification of the two ceramics treated by the CO_2 and the fibre laser was also believed to be influenced by the different laser wavelength and its absorption coefficient, the beam delivery system as well as the differences in the brightness of the two lasers used.

Keywords: CO_2 laser, Fibre laser, Si_3N_4 and ZrO_2 engineering ceramics, Vickers indentation method, K_{1C} .

1.0. Introduction

Low crack resistance and fracture toughness in comparison to metals can limit the use of ZrO_2 and Si_3N_4 engineering ceramics, particularly for demanding applications. In any case, the applications of ZrO_2 and Si_3N_4 have gradually increased on account of the desirable physical properties and longer functional life which often gives the engineering ceramics a commercial advantage over the conventional materials in use. Conventional metals and alloys especially can be replaced by engineering ceramics such as ZrO_2 and Si_3N_4 due to its exceptional mechanical and thermal properties offered. Now, ZrO_2 and Si_3N_4 ceramics in particular are predominantly being used to manufacture components in the aerospace, automotive and motorsports industrial sectors. For such applications, fracture toughness is an essential property since low fracture toughness in comparison to metals and alloys is one of the disadvantages of the ceramic. Inherently, an increase in the fracture toughness would therefore, lead to an enhancement in the components functional life, better performance which in turn leads to reduction in the maintenance time and cost of the component/part and or the system.

Fracture toughness is considered to be an important property for both of the ZrO_2 and the Si_3N_4 as well as other ceramics in general due to their high hardness and brittleness. Materials such as metals and alloys are soft and ductile which in turn would resist cracks at higher stress levels and loading [1, 2-4], whereas hard and brittle materials such as a Si_3N_4 ceramic possess a low fracture toughness and allow crack propagation to occur at lower stresses and loading. The fracture toughness for the ZrO_2 ceramic is fairly high in comparison to the Si_3N_4 but not in comparison to metals and alloys. This is due to their low ductility, high hardness, caused by the closely packed grains along

with a porous structure which increases the crack-sensitivity. This characteristically prevents these ceramics from increasing the movement of dislocations in comparison to that of metals [5-6]. Dislocations are hard to generate within the ceramics due to its strong and highly directional covalent bonds which make it difficult to move the atoms from its lattice positions. Mechanical yielding of the ZrO_2 or the Si_3N_4 is also limited due to the porosity and the surface flaws make it crack-sensitive and eventually lead to a much lower resistance to fracture. K_{Ic} is a parameter of fracture toughness and is low for both the ceramics in comparison with metals and alloys so it would be an advantage if the K_{Ic} of the ceramic is enhanced. Through improvement of K_{Ic} , it is possible to make way for new applications where metals and metal alloys fail due to their low hardness, thermal resistance, co-efficient of friction and wear rate.

This paper investigated the use of empirical equations from the literature to calculate the fracture toughness property (K_{Ic}) of a ZrO_2 and a Si_3N_4 engineering ceramic and observed the effects thereon of the CO_2 and the fibre laser surface treatment. A change in the K_{Ic} has an influence on the materials functionality or diversity to its applications, by improving the K_{Ic} of materials can enhance its functional capabilities such as longer functional life, improved performance under higher cyclic and mechanical loading particularly for demanding applications as previously mentioned.

Laser processing of ceramic based materials has been the subject of many investigations. Malshe *et al.* [7] investigated the CO_2 laser processing of a Si_3N_4 ceramic to eliminate imperfections within the ceramic and further conducted a three-point bending strength study of the Si_3N_4 after the CO_2 laser surface treatment. Sun Li *et al.* [8] then investigated that an YSiAlON phase within the Si_3N_4 was softened through melting and filled the pre-existing fractures to increase the flexural and the

bending strength. A similar investigation was also conducted by Segall *et al.* [9] by using a high powered CO₂ laser to cover a fractured surface of a thin film Al₂O₃ ceramic sheet. Nd:YAG laser machining of structural ceramics was demonstrated by Anoop *et al.* [10] and discussed the physical phenomenon of material removal of Al₂O₃, SiC, MgO and Si₃N₄ ceramics. The use of Nd:YAG laser was also employed by Hae and Lawrence [11] on MgO–PSZ ceramics to improve the wettability characteristics for biomedical applications. Hae and Lawrence [12] also investigated the improvement of cell adhesion through a CO₂ laser surface treatment. Hae and Lawrence [13] in another investigation used a finite element model (FEM) and compared it to an experimental model to simulate the CO₂ laser surface treatment of the MgO–PSZ. Several other studies discussed the use of industrial lasers to modify the surface of engineering, structural and refractory type ceramics [14 - 19]. Triantafyllidis *et al.* [14] investigated a possibility of achieving a crack-free surface of a refractory Al₂O₃ ceramics using double laser sources: a CO₂ and a high powered diode laser (HPDL) by balancing out the thermal gradient and increasing the solidification rate. Investigation by Lawrence and Li [15] initially employed a CO₂ laser; a Nd:YAG laser; a HPDL and an excimer laser with a SiO₂/Al₂O₃ ceramic to study the effect of the laser beam absorption on the ceramic and showed that the CO₂ laser had the highest absorption followed by the Nd:YAG and then the HPDL. Lawrence and Li [16] then employed a high powered diode laser (HPDL) to surface treat Al₂O₃ based refractory ceramic and achieved an increased wear life as a dense structure comprising of minor cracks and porosities were found. Another investigation by Lawrence and Li [17] also used the HPDL to process an ordinary Portland concrete (OPC) and showed enhancement in the resistance to chemical attack, water absorption as well as improved wear life of the OPC. Wang *et al.* [18, 19] published two separate papers on the micro-structural and surface density modification of a mixture of Al₂O₃ + ZrO₂ + SiO₂

refractory ceramics system from employing the CO₂ laser to show that the laser treatment had refined the microstructure into a fine grain dendrites structure as well as achieving a change in its phase transformation.

Much work has been conducted by using the CO₂, Nd:YAG, HPDL and an excimer to process various technical ceramics. However, no other investigation except the one of Shukla and Lawrence [20, 21] has been done hitherto by employing a fibre laser to process engineering ceramics. Moreover, the fibre laser was selected because of its shorter wavelength radiation in comparison to the conventional lasers previously used for ceramic processing [7-22]. Also the section of the CO₂ laser was made so a contrast of two different wavelengths can be seen. It would be interesting to investigate further the effect of short wavelength on the surface properties of the ZrO₂ and Si₃N₄ engineering ceramic. Moreover, Shukla and Lawrence [20-21] investigated the effects on the K_{1c} using a fibre laser to surface treat a ZrO₂ and Si₃N₄ engineering ceramics which showed changes in the K_{1c} of the both ceramics. However, the effects of the fibre laser are different to that of the CO₂ laser due to the differing wavelength, beam conditions as well as the beam delivery system despite applying identical parameters. This is why a broader investigation was carried out by using the CO₂ and the fibre laser on the ZrO₂ and the Si₃N₄ engineering ceramic. Furthermore, despite the Nd:YAG laser wavelength being in the same region as that of the fibre laser, the Nd:YAG laser does not function stably in the continuous wave (CW) mode. This is required for reducing the thermal shock induced into a ceramic. Fibre lasers also produces high brightness in comparison to the more conventional CO₂ and Nd:YAG lasers which generally inhibits deeper penetration, capability of producing finer spot sizes, longer depth of focus, as well as low cost per wattage being exhibited due to it high brightness. As one can see, this investigation is timely as limited research has been conducted by employing fibre

lasers to conduct the surface treatment of materials, particularly for engineering ceramics.

2.0. Background of the Vickers indentation method to determine the K_{1C} of the ceramics

The Vickers indentation test can be used to determine the K_{1C} of ceramics and glass type materials from empirical relationships as demonstrated in [1, 2, 4, 23 - 25]. The procedure and steps in order to produce a genuine Vickers indentation test was followed and is documented elsewhere [26]. Several authors have used this method to determine the K_{1C} of ceramics and glass type materials [3, 4, 20, 21, 27, 28]. Ponton and Rawlings [3, 4] Chicot *et al.* [24], Liang *et al.* [25], Orange *et al.* [28] presented a thorough investigation into various equations specifically applied to ceramics and justified the reasons for their suitability for use. The equations originate from various other authors [27, 29-38] and are said to be unique for various ceramics and glass based materials. However, due to simplicity and ease of use, equations derived by Ponton and Rawlings were adopted for this investigation.

3.0. Experimentation Technique and Analysis

3.1. Background of the test materials

The materials used for this work was a Cold Isostatic Pressed (CIP) Si_3N_4 with (90% Si_3N_4 , 4% Ytria, 4% Al_2O_3 (alumina) and 2% other unspecified content by the manufacturer) and ZrO_2 with (95 % ZrO_2 and 5 % Ytria). Each test piece was 10 mm x 10 mm x 50 mm bars and comprised the surface roughness of $1.56\mu m$ (Si_3N_4) and $1.58\mu m$ (ZrO_2) ceramics as provided by the manufacturer (Tensky International Company Ltd; Taiwan). This was to minimize the beam reflection as shinier surfaces

would reduce beam absorption, although, rougher surfaces of the ceramics can often be more prone to cracking in comparison [1, 39]. The experiments were conducted in ambient condition at a known atmospheric temperature (20°C). All surfaces of both the Si₃N₄ and ZrO₂ engineering ceramics to be treated were marked with black ink prior to the laser treatment to enhance the absorption and allow the laser beam to further penetrate into the surface. Initial experiments reviewed that the black ink helped the beam to absorb better into the material. This was particularly the case with the ZrO₂ ceramic as it reflected the beam without the black ink because of its colour being white. Furthermore, it was necessary to conduct like by like experiments with both lasers types using identical material surface conditions so a true comparison of the effects of the two lasers can then be further performed. The black ink was generally removed by the CO₂ or the fibre laser surface treatment and was not found to have any further effect on the ceramics after the laser surface interaction had taken place.

3.2. Vickers indentation test

An indenter of a specific shape made from a diamond material was used to indent the CO₂ and the fibre laser treated surfaces of the Si₃N₄ and the ZrO₂ engineering ceramics. Around 50 indentation tests each were performed on all surfaces examined. An indentation load of 49.05 N was used. The indented surface and the resulting crack lengths were measured using the optical microscopy and a co-ordinate measuring machine. A standardized technique was adopted to ensure that a valid indentation tests were performed [26]. Thereafter, the surface area of the indentation (diamond footprint) was placed into Equation 1 to calculate the hardness value:

$$HV = 2P \sin [\theta/2] / D^2 = 1.8544P/D^2 \quad (1)$$

where, P is the applied load, D is the average diagonal size of the indentation and θ is the angle between the opposite faces of the diamond indenter.

3.3. Calculation of the K_{IC}

The equation used to determine the K_{IC} in this work was chosen by taking in consideration of the findings in a previous investigation by Shukla and Lawrence [20], which revealed that Palmqvist cracks were produced followed by a propagation of the median half-penny cracks when applying a high indentation loads to the as-received surface of the ceramics. Furthermore, the values produced by this equation was 38% accurate for the Si_3N_4 and 42% for the ZrO_2 in obtaining the true K_{IC} values which is usually between 4 to 8 MPa $m^{1/2}$ for the Si_3N_4 and 8 to 12 MPa $m^{1/2}$ for the ZrO_2 ceramic. Equation 2 was hence used based on these finding to calculate the K_{IC} of all laser treated ceramic samples in this study.

$$K_{IC} = 0.016 (E/HV)^{1/2} (P/c^{3/2}) \quad [3] \quad (2)$$

Where, P is the load; c is crack length; HV is the Vickers material hardness value; E is Young's modulus (320 GPa for the Si_3N_4 and 210 GPa for the ZrO_2) and 0.016 is the materials empirical value [3, 4]. The hardness obtained from the Vickers indentations test and the crack length of the ceramics after the Vickers indentation test were the changing input parameters for Equation (2).

3.4. CO₂ laser surface treatment

A 1.5 kW CO₂ laser (Everlase S48; Coherent, Ltd.) emitting at a wavelength of 10.6 μm in the continuous wave (CW) mode was used in this work. The processing gas used was compressed air, at a flow rate of 25 litre/min. To obtain an operating window,

trials were conducted by varying the power between 50 to 200 W and varying the traverse speed between 100 and 600 mm/min. From these trials it was found that 65 W at 600 mm min/min for ZrO₂ and 175 W at 100 mm/min for Si₃N₄ were the ideal laser parameter to use in terms of achieving a crack-free surface. Stand-off distance between the nozzle and the work-piece was kept to 16 mm in order to obtain a focal spot size of 3 mm. Programming of the laser was conducted using an integrated software which controlled the motion system. A 50 mm line was programmed using numerical control (NC) programming as a potential beam path which was transferred by a .dxf file.

3.5. Fibre laser surface treatment

A 200 W fibre laser (SP-200c-002; SPI, Ltd.) was employed which emitted a continuous wave (CW) mode beam at a wavelength of 1.075 µm. The processing gas used was compressed air and was supplied at a flow rate of 25 litre/min. To obtain an operating window, trials were conducted at a fixed spot size of 3 mm and by varying the power between 25 and 200 W, as well as varying the traverse speed between 25 and 500 mm/min. From these trials, it was found that 143 W at 100 mm/min for the ZrO₂ and 200 W at 100 mm/min for the Si₃N₄ were the ideal laser parameter to use in terms of achieving a crack-free surface. A 50 mm line was also programmed using NC programming as a potential beam path which was transferred by a .dxf file.

4.0. Results and Discussion

4.1. Comparison of CO₂ laser surface treatment with fibre laser surface treatment of the ZrO₂ engineering ceramic

4.1.1 Change in the surface hardness

Figure 3 presents the fluctuations in the hardness of the CO₂ and the fibre laser radiated surfaces of the ZrO₂ ceramics along with its mean hardness value over 50 indentation tests that were conducted on one surface plane. As one can see that the hardness of the CO₂ laser radiated surfaces was considerably lower than that of the fibre laser radiated surface. The average hardness of the CO₂ laser radiated ZrO₂ was 854 HV with the highest value being 1120 HV and the lowest being 473 HV. The average hardness for the fibre laser radiated surface of the ZrO₂ was 940 HV. The highest value above the mean was 1089 HV and the lowest being 826 HV for the ZrO₂ ceramic. The hardness values fluctuated in both of the curves due to an uneven surface being produced from material removal as well as melting and solidification. The hardness of the CO₂ laser radiated surface was up to 22% lower than that of the fibre laser. This showed that the CO₂ laser radiation had softened the surface of the ZrO₂ in comparison to that of the fibre laser radiated surface.

4.1.2. Change in the crack length

Average crack length of the CO₂ laser treated surfaces was 216µm with the highest value above the mean being 333µm and the lowest being 143µm as presented in Figure 4. The average crack length of the fibre laser radiated surface of the ZrO₂ was 171µm. The crack length was much reduced in comparison with the crack length of the CO₂ laser radiated surfaces. Despite the increase in hardness produced by the fibre laser radiated surface, a 21% decrease in crack length was found from the fibre laser

radiation. This can be seen from Figure 5 and Figure 6 where the diamond indentation produced by the CO₂ laser radiation (see Figure 5) was larger due to the softening of the surface but produced high cracking profiles. In comparison, the indentation created by the fibre laser radiated surface was smaller due to surface hardening and yet produced a considerably smaller cracking geometry. The expected result was larger crack length due to smaller indentation foot-print produced. From this, it can be postulated that compressive residual stress could have been induced during the fibre laser surface radiation which caused lower crack propagation as further explained in section 4.3.

One can see from the optical micrographs in Figure 5 and Figure 6 that surface oxidation is not apparent. The ZrO₂ ceramic is less sensitive to the effect of surface oxidation during the exposure to the laser beam radiation due to the majority of the ZrO₂ ceramics comprising of Zr + O₂. It can also be seen from the optical micrographs that the ZrO₂ has been changed in colour especially in Figure 5 due to the thermal energy being induced. It is possible however, that the ZrO₂ had undergone a degree of compositional change since it has been exposed to the environment at high temperatures during both CO₂ and the fibre laser irradiation. A compositional change from ZrO₂ to ZrCO₂ is likely to have occurred during the laser surface interaction. This would bring changes in the fracture resistance of the ZrO₂ and is deemed to have influenced the K_{1C} values after the laser surface treatments.

4.1.3. Change in the surface K_{1C}

Figure 7 presents the K_{1C} of the CO₂ and the fibre laser treated ZrO₂ ceramics which showed that the K_{1C} of the fibre laser radiated surfaces was 29% higher than that of the CO₂ laser radiated surface. The average K_{1C} of the CO₂ laser radiated surface of the

ZrO₂ was 5.63 MPa m^{1/2} with the highest value being 9.85 MPa m^{1/2} above the mean and the lowest being 2.97 MPa m^{1/2} below the mean. The average value found for the CO₂ laser radiated surface of the ZrO₂ was 4.16 MPa m^{1/2} with the highest value being 7.54 MPa m^{1/2} and the lowest being 1.89 MPa m^{1/2}. The values for both laser treated surfaces fluctuated due to the variation in the surface hardness and the differing crack geometries. The surface finish of the ceramics prior to the laser treatment should also be considered where the unpolished (as-received) surface is more prone to cracking during the diamond indentation due to pre-existing manufacturing surface flaws and micro-cracks which was the case in the study.

4.2. Comparison of CO₂ laser surface treatment and fibre laser surface treatment of the Si₃N₄ engineering ceramic

4.2.1. Change in the surface hardness

The average hardness of the CO₂ laser radiated surface of the Si₃N₄ was 1028 HV which was - a reduction of 13% from the fibre laser radiated surface (1154 HV). This reduction in the surface hardness indicated that a softer surface layer was also produced by the CO₂ laser radiation in comparison to that of the fibre laser radiation. The hardness values ranged between 264 and 1449 HV for the CO₂ laser radiated Si₃N₄ and between 788 HV to 1449 HV for the fibre laser radiated Si₃N₄ as shown in Figure 8. It is evident from Figure 8 that the fluctuation in the hardness value was large. The reason for this was due to the surface containing an oxide layer of around 100 to 150µm thickness resulting from both laser treatments which was somewhat softer and more uneven in comparison to the laser unaffected surface. As such, the diamond indenter

penetrated deeper into the surface in some of the regions than in others, which is why the diamond indentation in Figure 9 and Figure 10 are not symmetrical.

Figure 9 and Figure 10 presents an example of a diamond indentation produced and the accompanying crack geometry. It can be seen from the two images that the diamond indentation produced on the CO₂ laser radiated Si₃N₄ (see Figure 9) is larger than that of the fibre laser radiated surface (see Figure 10). Both the CO₂ and the fibre laser treated surface of the Si₃N₄ genuinely showed evidence of surface oxidation. The new surface was formed from the result of the Si₃N₄ ceramic being exposed to the atmosphere at high temperatures. This would have led to the possible compositional change where the Si₃N₄ was changed to SiO₂. Moreover, the occurrence of the white phase as illustrated in Figure 9 and 10 would also lead to some modification in the micro-structure of the Si₃N₄ ceramic as the white oxide layer would be formed above the normal surface of the Si₃N₄ which in turn would generate in-filling of the surface cracks in various areas and also cover the grains that would normally appear on the top surface layer. The change in composition of the Si₃N₄ was also confirmed from a previous investigation by Lysenko *et al.* [40]. A reduction in the crack length obtained on the CO₂ laser radiated surface occurred due to the oxide layer being somewhat thicker in various areas in comparison which showed lower surface hardness and the resulting crack lengths.

4.2.2. Change in the crack length

The crack lengths obtained from both of the laser radiated surfaces are presented in Figure 11. The average crack length obtained from the CO₂ laser radiation was 210µm and ranged between 135 to 295µm. This in comparison to the cracks produced by the Vickers indentation test of the fibre laser radiated Si₃N₄ was 16% lower. An average

crack length found was 242 μm with a highest of 337 μm and the lowest of 164 μm for the fibre laser radiated surfaces. The fluctuation from the values in Figure 11 has resulted from the newly formed, uneven oxide layer after both of the laser surface treatments.

4.2.3. Change in the K_{1C}

The average K_{1C} of the CO_2 laser treated surface was found to be 4.78 $\text{MPa m}^{1/2}$ and ranged between 2.74 $\text{MPa m}^{1/2}$ and 11.90 $\text{MPa m}^{1/2}$. This was 26% higher in comparison to that of the fibre laser radiated surface of the Si_3N_4 ceramic. The average K_{1C} value for the Si_3N_4 after the fibre laser treatment was 3.51 $\text{MPa m}^{1/2}$. The highest K_{1C} value obtained above the mean was 6.03 $\text{MPa m}^{1/2}$. The results are shown in Figure 12. The values also fluctuate considerably due to the variations found in the hardness and the crack lengths that led to generating an uneven surface profile as mentioned earlier in this study.

4.3. Differences between the CO_2 and the fibre laser surface treatment and the effects on the hardness, crack lengths and the K_{1C} of the engineering ceramics.

4.3.1. Rationale for the change in the hardness

The results showed that a change in the hardness occurred from both of the laser treatments to the ZrO_2 and the Si_3N_4 engineering ceramics. However, the hardness produced by the CO_2 laser in comparison to the fibre laser was somewhat lower. This was due to the difference in the absorption of the mid infra-red wavelength CO_2 and the near infra-red wavelength of the fibre laser wavelength. Both the CO_2 and the fibre

laser wavelength, however, penetrate to a significant depth within the ceramics. Although, the CO₂ laser has the tendency to produced high interaction zones at the surface where as the fibre laser is penetrated deeper into the ceramic layer for the Si₃N₄ ceramic in particular. This produces more compositional change at the top surface radiated by the CO₂ laser as the white SiO₂ layer is produced which is somewhat softer in comparison to the parent surface. For the ZrO₂ ceramic, the fibre laser wavelength is somewhat transparent hence, the interaction is lower in comparison to the CO₂ laser interaction with the ZrO₂. This in turn will produced high local temperature and larger melt pool at the surface but yet it is still shallow in comparison to the fibre laser radiated surface. The larger melt zone intrinsically produces a bigger diamond indentation foot-print in comparison to the fibre laser radiated surface and therefore has slightly lower hardness in comparison. This finding relate to the work of White *et al.* [41] who reported that an increase in the hardness of boron carbide ceramic by processing with the near infra-red wavelength of a Nd:YAG laser was found which comply with the higher hardness found with the near infra-red wavelength of the fibre laser.

Furthermore, taking into consideration of the effects produced by laser float zone (LFZ) melting and (LZM) of eutectic ceramics by several workers [41-49], it can be said that considerable change in the microstructure would occur after the laser material interaction has taken place with both the CO₂ and the fibre laser radiated ceramics in this work. Those changes are within the surface morphology, growth of oxide crystals, and changes in the grain size and direction would occur, formation of amorphous layers as well as decrease in porosity would occur which in turn would considerably affect the local characteristics and properties of the ceramics particularly in the case of the

surface hardness and the K_{Ic} which heavily influences the microstructure of the ceramics. Further investigation are being undertaken to justify the micro-structural modifications induced by the laser surface treatment.

4.3.2. Rationale for the change in the crack lengths and the end K_{Ic} of the ceramics

The increase in the hardness usually manifests as an increase in the crack length due to the ceramic becoming more brittle; however, this did not occur with surfaces of both CO_2 and the fibre laser radiation. A likely cause for this would be the effect of crack healing as the pre-existing surface micro-cracks on the ceramic were filled and covered particularly by the fibre laser radiation. Also, the event of phase transformation would have occurred for both ceramics which led to a change in the K_{Ic} values.

Consideration must also be given to the event of strain hardening taking place as a result of the fibre laser-ceramic surface interaction. The effect of strain hardening through movement of dislocations at elevated temperatures inherently could induce compression into the surface and sub-surface of the ceramic and through the effect of transformation hardening. If one considers the heat generated from irradiation by the fibre laser beam is likely to have caused the Si_3N_4 in particular to transform from the α to β state at 1600 °C, as stated by Jiang *et al.* [50]. This intrinsically would have caused the observed increase in the hardness of the Si_3N_4 to 3600 HV in particular. Since, the temperature during the fibre laser processing has been found to be much higher than 1600°C [50] for both ceramics, phase transformation of $\alpha - \beta$ phase will inherently

occur within the Si_3N_4 and from monoclinic (M) phase to active tetragonal (T) phase would occur within ZrO_2 during the fibre laser irradiation.

An investigation by Moon *et al.* [51] found that the fracture toughness of Al_2O_3 and Si_3N_4 ceramics was improved considerably by generating dislocations within the ceramics by plastic deformation (shot blasting) and then annealing to temperatures of 1500°C . Work by Shukla and Lawrence [21] showed that the fibre laser surface processing of the Si_3N_4 and the ZrO_2 occurred above 2000°C and could have led to an increase in the hardness as the movement of dislocations at high temperatures would have induced a degree of residual stress into the ceramic in the form of compression.

In account of the fibre laser induced compression (see Figure 13), the tension would have needed to overcome the compression in order to propagate a crack. Therefore, the cracking of the ceramics was much smaller with the fibre laser radiated surface in comparison to that of the CO_2 laser radiation. This meant that the tension induced by the 49.05 N load to produce a crack on the fibre laser treated surface was much smaller than the induced compression. This rational goes some way to explaining the reason why smaller crack lengths have been found on the fibre laser treated ceramic (particularly with Si_3N_4) surfaces in comparison with the CO_2 laser treated surface. Values obtained for the hardness, crack length and the K_{1C} for the Si_3N_4 and the ZrO_2 ceramics treated by both the fibre laser and the CO_2 laser are presented in Table 1.

4.4. Other influential aspects affecting the K_{IC} of the laser treated ceramics

4.4.1. Differences in laser parameters

The differences within the K_{IC} results achieved by the CO_2 and the fibre laser surface treatment have occurred due to several aspects which should be considered. Those are the material absorption; laser beam delivery system; wavelength and the brightness (power per unit area). The beam quality of the CO_2 laser and the fibre laser are in the same region (TEM_{00}). Therefore, the effect of the beam quality factor is minimal. However, it is important to consider the way in which the Gaussian beam of TEM_{00} is delivered as this would have an influence on the interaction between the ceramics and the specific laser used. Since the CO_2 laser is delivered by a galvanometers and stationary mirrors the beam is focused at a fine spot size whereas the fibre laser beam is delivered by a fibre cable which is less focused. It is required that a larger beam size is used for ceramic surface treatment so that the laser beam is distributed evenly onto the ceramic. In this, case a fibre laser with a low focused beam in comparison to that of the CO_2 would be more ideal especially for the surface treatment of the ceramics.

The material absorption co-efficient is varied with different laser wavelengths. As some wavelength are better absorbed by the ceramics than others. The CO_2 laser wavelength absorption with ceramics is about 87% whereas the fibre laser wavelength absorption is about 92%. This means that the fibre laser wavelength is more absorbed into the material and exhibits better interaction zone. This produces more photon energy that is induced onto the ceramic surface. This in turn, produces high temperatures during the fibre laser processing which allows the ceramics to undergo phase and compositional changes and affect the hardness and the resulting crack

geometries in different ways and has also affected the end K_{IC} result from the two different laser sources used.

The difference in the laser brightness (luminance) between the two lasers used would also have an effect during the ceramic interaction as the fibre laser is much brighter than the CO_2 laser which indicates that there is more power per unit area being executed at the ceramic surface. On account of this, it is indicative that the luminance at high power per unit area is larger with the fibre laser and produces more interaction, high processing temperatures and rather leads to transformation hardening of the ceramics which is not seen with the CO_2 laser surface radiation.

4.4.2. Influence of the ceramics surface condition

The CO_2 and the fibre laser both were executed on the as-received surfaces of the ZrO_2 and the Si_3N_4 ceramics which comprised of some degree of surface flaws such as porosity and micro cracks and machine induced scaring. Due to this, the possibility of crack propagation increases during the diamond indentation tests. If the surface flaws were minimized in this study by introducing grinding and polishing of the near surface layer of the ceramics then the crack propagation during the indentation test would have been somewhat low. This is also true because the ground and polished surfaces are free from the surface impurities and has the tendency to induce compressive stress and allow the ceramics to be more resistant to cracking [39]. This in turn, also increases the surface K_{IC} as the resulting crack lengths from the indentation tests are reduced which also indicate that the surface of the ceramics are less prone to cracking.

4.4.3. Effects of phase transformation and change in composition

A new surface was formed especially on the top surface of the Si_3N_4 ceramic after being radiated by both CO_2 and the fibre laser (see Figure 9 and Figure 10). This was because of the Si_3N_4 ceramic being exposed to the atmosphere at high temperatures and led to a possible change in the composition as the Si_3N_4 was changed to SiO_2 . Consequently, the effects with ZrO_2 were also identical after conducting both the CO_2 and the fibre laser surface treatments. A change in composition within the ZrO_2 would have also taken place where the top surface of the ZrO_2 was changed to ZrCO_2 . A compositional change within the laser radiated ZrO_2 and Si_3N_4 was also previously confirmed with the work of Shukla and Lawrence [52]. A change in composition after the fibre laser surface treatment in turn, would affect the hardness of the ceramics which inherently influenced the crack geometry during the Vickers indentation test and furthermore, the end K_{1C} values.

4.4.4. Effects of the Vickers indentation test and parameters used within the K_{1C} equation

The Vickers indentation method is easy to set-up and cost effective but it still has several flaws such as the results obtained from the hardness test heavily depending on user's ability to detect the crack lengths and its geometry. The K_{1C} values could be much improved if the surface hardness values and the resulting crack geometries were consistently balanced with minimal fluctuation. The fluctuations found in the mean hardness from the results of this study were up to 11 %. This in comparison with the values for the ceramics given in the literature were 1 % higher from the ± 10 % range (error) given in [2]. Error of at least 1 % (minimum) between the hardness values found in this study and the literature can be an exempt from being a non- conformance and may be considered to pass through the quality requirements if the hardness test was used for a (real life) ZrO_2 ceramic engineering component/product. This could be found from adopting other indentation methods and by using many of the other existing empirical equations.

Calculation of fracture toughness is somewhat difficult due to various uncertainties such as the selection of the most appropriate equation; input parameters which compliment the equation used; the surface conditions of the ceramics and the ceramics response to the diamond indentations. Consideration should be given to two parameters that can influence the K_{IC} of the ceramics here in this investigation and on a general note. Those parameters are; the indentation load and the Young's modulus. Whereas the indentation load was kept constant in this study, so the effects of this parameter were zero. However, the Young's modulus would also influence the K_{IC} of the Si_3N_4 since an increase in the ratio of stress and strain which in turn increases the Young's modulus value and affects the end K_{IC} value. If the effect of Young's modulus was ignored then the K_{IC} value for the CO_2 laser treated surfaces would be reduced to 6% on average.

5.0. Conclusions

Fracture toughness property (K_{1C}) of the ZrO_2 and Si_3N_4 engineering ceramics was conducted following a CO_2 and a fibre laser surface treatment. Vickers indentation technique was employed for determination of K_{1C} . The following conclusions were found from comparing the two laser sources applied to the ZrO_2 and the Si_3N_4 ceramics:

- The CO_2 laser radiated surfaces in comparison to the that of the fibre laser radiated surface modified the K_{1C} of both ceramics was found by the CO_2 and the fibre laser surface treatment in comparison to the as-received surfaces.
- The K_{1C} values found on the CO_2 laser radiated surface of the Si_3N_4 was 3 % higher in comparison to that of the fibre laser. This was due to the near surface of the Si_3N_4 being soft and was lower in hardness which further increased the fracture resistance.
- The effects were different with the ZrO_2 ceramic to that of the Si_3N_4 as the fibre laser surface treatment on this occasion had produced a rise of 34% compared to that of the CO_2 laser radiation. This was because of low crack propagation which resulted from the Vickers indentation test and inherently affected the end K_{1C} of the fibre laser radiated surface of the ZrO_2 engineering ceramic.
- The K_{1C} modification of the two ceramics treated by the CO_2 and the fibre laser was also believed to be influenced by the different laser wavelengths and its absorption co-efficient of the ceramics as well as the beam delivery system and the brightness of the two laser types applied.

- The change in wavelength affects the absorption of the laser energy. The fibre laser was induced deeper into the surface of the ceramics in particular the Si_3N_4 whilst the CO_2 laser produced larger profile and more broader laser affected region which in turn generated a larger oxide layer which was somewhat softer in comparison to the fibre laser radiated surface.
- For the ZrO_2 ceramic, the fibre laser wavelength was somewhat transparent so the laser-material interaction was lower in comparison to the CO_2 laser interaction with the ZrO_2 . High local temperature and larger melt pool at the surface were therefore produced. Furthermore, the larger melt zone produced a bigger diamond indentation foot-print in comparison to the fibre laser radiated surface and comprised of slightly lower hardness in comparison.

6.0. References

1. Shukla PP. *Laser Surface Treatment of Silicon Nitride*. MSc by Research thesis Coventry University; 2007.
2. McColm IJ. *Ceramic Hardness*. New York: Platinum Press, 1990.
3. Ponton B, Rawlings C. Vickers indentation fracture toughness test, Part 1 - Review of literature and formulation of standardised indentation toughness equations. *Journal of Materials Science Technology* 1989; **5**: 865- 872.
4. Ponton B, Rawlings C. Vickers indentation fracture toughness test, Part 2 - Review of literature and formulation of standardised indentation toughness equations. *Journal of Materials Science Technology* 1989; **5**: 961- 976.
5. Mitczell TE. Dislocations in Ceramics. *Journal of Materials Science and Technology* 1985; **1**: 994 – 949.
6. Castaing J, Veyssiere, P. *Core Structure Dislocations in Ceramics*. Gordon and Breach Science Publishers Inc and OPA Ltd U.K 1985; **12**: 213 -227.
7. Malshe A, Sun Li, Jiang W, McCluskey WP. Effect of CO₂ Laser Surface Processing on Fracture Behaviour of silicon Nitride Ceramic. *Journal of engineering materials and technology* 2006; **128**: 460 – 467.
8. Sun Li, Malshe AP, Wen-ping Jian, Mccluskey PH. Experimental investigation of laser surface processing of flexure silicon nitride ceramic. *Transactions of Nonferrous Materials Society of China* 2006; **16**; 558-565.
9. Segall AE, Cai G, Akarapu R, Ramasco A. Fracture control of unsupported ceramics during laser machining using a simultaneous prescore. *Journal of Laser Applications* 2005; **17** (Issue 1): 57-62.

10. Anoop N, Samant B, Narendra, Dahotre. Differences in physical phenomena governing laser machining of structural ceramics. *Ceramics International* 2009; **35**; 2093–2097.
11. Hae L, Lawrence J. Effects of Nd:YAG laser treatment on the wettability characteristics of a zirconia-based bioceramic. *Optics and lasers in engineering* 2006; **44**; 803- 814.
12. Hae L, Lawrence J, Chian KS. Osteoblast cell adhesion on a laser modified zirconia based bioceramic. *Journal of Material Science: Materials in Medicine* 2005; **16**; 719– 726.
13. Hao L, Lawrence J. Numerical modeling of the laser surface processing of magnesia partially stabilized zirconia by the means of three-dimensional transient finite element analysis. *Proceedings of the Royal Society-A* 2006; **462** (no 2065): 43-57.
14. Triantafyllidis D, Li L, Stott FH. Surface treatment of alumina-based ceramics using combined laser sources. *Applied surface science* 2002; **186**: 140 – 144
15. Lawrence J, Li L. On the Differences between the Beam Interaction Characteristics of CO₂, Nd:YAG, Excimer and High Power Diode Lasers with a SiO₂ /Al₂O₃ Ceramic. *Lasers in Engineering* 2002; **12 (Issue 2)**; 81–93
16. Lawrence J, Li L. Augmentation of the mechanical and chemical resistance characteristics of an Al₂O₃-based refractory by means of high power diode laser surface treatment. *Journal of Materials Processing Technology* 2003; **142**: 461 – 465.

17. Lawrence J, Li L. The enamelling of concrete for improved performance characteristics by means of high power diode laser interaction. *Journal of Materials Processing Technology* 2003; **138**: 551–559
18. Wang HA, Wang WY, Xie CS, Song WL, Zeng DW. CO₂ laser-induced structure changes on an alumina–mullite–zirconia refractory. *Applied Surface Science* 2004; **223**: 244 – 251
19. Wang HA, Wang WY, Xie CS, Song WL, Zeng DW. Micro-structural characteristics of Al₂O₃-based refractory containing ZrO₂ induced by CO₂ laser melting. *Applied surface Science* 2003; **221**: 291- 301.
20. Shukla PP, Lawrence J, Wu H. On the Fracture Toughness of a Zirconia Engineering Ceramic and the Effects thereon of surface processing with fibre laser radiation. *Proceedings of the IMechE Part B* 2009; **224**: (in press) DOI: [10.1243/09544054JEM1887](https://doi.org/10.1243/09544054JEM1887)
21. Shukla PP, Lawrence J, Fracture Toughness modification by using a Fibre Laser Surface Treatment of a Silicon Nitride Engineering Ceramic, *Journal of Materials Science* 2010; (in press). **45 (21)**: (in press) DOI: [10.1007/s10853-010-4743-6](https://doi.org/10.1007/s10853-010-4743-6)
22. Lawrence J, Li L, On The difference between the beam interactions characteristics of CO₂, Nd: YAG Excimer and high powered diode lasers with a SiO₂/Al₂O₃ ceramic. *Lasers In Engineering* 2002, **12**; No. 2: 81 – 93.
23. Lawn BR, Evans AG, Marshall DB. Elastic/ Plastic Indentation Damage in ceramic: The Median/ Radial Crack System. *Journal of American Ceramic Society* 1980; **63 (9-10)**: 574 – 581.

24. Chicot D. New Development for fracture toughness determination by Vickers indentation. *Journal of Materials Science and Technology* 2004; **20**: 877- 884.
25. Liang KM, Orange G, Fantozzi G. Crack resistance and fracture toughness of Alumina and Zirconia ceramics: Comparison of notched-beam and indentation technique. *Science Ceramics 14th International Conference*, 1988; **14**: 709- 714.
26. British Standards, *Vickers Hardness Test- Part 2- Verification and Calibration of testing Machines*. Metallic Materials - ISO 6507-1; 2005.
27. Exner HE. The Influence of Sample Preparation on Palmqvist's Method for Toughness Testing of Cemented Carbides. *Transactions of the Metallurgical Society of AIME*, 1989; **245** (4): 677 – 683.
28. Orange G, Liang KM, Fantozzi G. Crack Resistance and fracture toughness of alumina and Zirconia ceramics: comparison of notched beam and indentation technique. *Science of ceramics* 14, 1987; **PT 7 – 9**: 709 – 14.
29. Marion RH. *In fracture mechanics applied to brittle materials*. STP 678 (Ed S. W Freiman) 103 – 111, Philadelphia, PA, ASTM 1979.
30. Evans AG, Wilshaw TR. Quasi static particle damage in brittle solids. *Acta Metall* 1976; **24**: 939 – 956.
31. Evans AG, Charles EA. Fracture Toughness Determinations by Indentation. *Journal of American Society* 1976, **59** (7 – 8): 371 – 372.
32. Lawn BR, Evans AG, Marshall DB. Elastic/ Plastic Indentation Damage in ceramic: The Median/ Radial Crack System. *Journal of American Ceramic Society* 1980; **63** (9–10); 574 – 581.

33. Marshall DB. Failure from contact induced surface flaws. *Journal of American Ceramic Society* 1983; **66**; 127 – 131.
34. Anstis GR, Chanrikul P, Lawn BR, Marshall DB. *Journal of American Ceramic Society* 1981; **64**: 533 – 538.
35. Niihara K, Morena R, Hasselman DPH. Evaluation of K_{IC} of brittle solids by the indentation method with low crack-to-indent ratios. *Journal of material Science Literature* 1982; **1**: 13 – 16.
36. Tani T, Miyamoto Y, Koizumi M. Grain Size Dependences of Vickers microhardness and fracture toughness in Al_2O_3 and Y_2O_3 ceramics. *Ceramics International* 1986; **12**: 33 – 37.
37. Hoshide T. Grain fracture model and its application to strength evaluation in engineering ceramics. *Engineering fracture mechanics* 1993; **44** (No 3); 403 – 408.
38. Kelly JR, Cohen ME, Tesk JA. Error Biases in the Calculation of Indentation fracture Toughness for Ceramics. *Journal of American Ceramic Society* 1993; **76** (10): 2665 – 2668.
39. Ahn Y, Chandrasekar S, Farris TN. Determination of Surface residual stress in machined ceramics using indentation Fracture. *Journal of Manufacturing Science and Engineering* 1996; **118**: 483 – 489.
40. Lysenko VS, Nazarov AN, Lokshin MM, Kaschieva SB. Effects of laser irradiation on the structure of silicon dioxide film with implanted phosphorus ions. *Fiz. Tekh. Poluprovodn* 1977; **1** (11): 2254-2257.

41. White RM, Kunkle JM, Polotai AV, Dickey EC, Microstructure and hardness scaling in laser-processed B₄C–TiB₂ eutectic ceramics, *Journal of the European Ceramic Society* 2010; (in press).
42. Brody HD, Haggerty JS, Cima MJ, Flemings MC. Highly Textured and single crystal Bi₂CaSr₂Cu₂O_x prepared by laser heated float zone crystallization. *Journal of Crystal Growth* 1989; **96**: 225—233.
43. Ozkan N, Glowacki BA, Robinson EA, Freeman PA, Infrared zone melting process for YBa₂Cu₃O_{7-δ} wires. *Journal of Materials Research* 1991; **6**: 1829 – 1837.
44. Pena JI, Merino RI, Harlan NR, Larrea A, Fuente de la GF, Orera VM, Microstructure of Y₂O₃ doped Al₂O₃–ZrO₂ eutectics grown by the laser floating zone method. *Journal of the European Ceramic Society* 2002; **22**: 2595–2602
45. Lennikova VV, Kazin PE, Tretyakov YD, and Fuente de la GF, Laser Zone Melting and Texture Formation in MgO-doped Bi_{2.03}Sr_{1.93}Ca_{1.07}Cu_{2.05}O_{8+δ} *Journal of Inorganic and General Chemistry* 2002, **630**: 2337-2342
46. Larrea A, Fuente de la GF, Merino RI, Orera VM, ZrO₂–Al₂O₃ eutectic plates produced by laser zone melting, *Journal of European Ceramic Society* 2002; **22**: 191 - 198
47. Leral F, Angurel LA, Rojo JA, Moral M, Recuero S, Arroyo MP, Andrés N, Microstructure origin of hot spots in textured laser zone melting Bi-2212 Monoliths. *Institute of Physics Publishing, Superconductor Science and Technology*, 2005, **18**: 1489 - 1495

48. Su H, Zhang J, Liu L, Fu H, Processing, microstructure, and properties of laser remelted $\text{Al}_2\text{O}_3/\text{Y}_3\text{Al}_5\text{O}_{12}$ (YAG) eutectic in situ composite, *Transition of nonferrous material society of China*, 2007: **17**; 1259-1264
49. Angurel LA, Carlos Diez J, Francisco de la Fuente G, Laser Induced Cylindrical Zone Melting of $\text{Bi}_2\text{Sr}_2\text{CaCu}_2\text{O}_{8+\delta}$ Superconductors, *Journal of Inorganic and General Chemistry*, 2009; **635**: 1767 – 1772.
50. Jiang JZ, Kragh F, Frost DJ, Stahl K, Lindelov H, Hardness and thermal stability of cubic silicon nitride. *Journal of physics condensed matter* 2001: **13** (No 22): L515-L520.
51. Moon W, Ito T, Uchimura S, Saka H. Toughening of ceramics by dislocation sub-boundaries. *Material Science and Engineering A* 2004: **387 – 389**; 837 – 839.
52. Shukla PP, Lawrence J. Characterization of fibre laser treated engineering ceramics. *Proceedings of ICALEO-09 FL (USA)*; 2009.

7.0. Nomenclature

Alumina	Al_2O_3
Average diagonal size	D
Average Flaw Size	c
Beta	β
Cold Isostatic Pressed	CIP
Co-Ordinate Measuring Machine	CMM
Degrees Centigrade	$^{\circ}\text{C}$
Delta	δ
Fracture Toughness	K_{1C}
Giga Pascal	GPa
Hardness	HV
Hot Isostatic Pressed	HIP
Interior Cracks	Ic
Litres	l
Load (Kg)	P
Load Impact	Pc
Mega Pascal	MPa
Meter Cubed	m^3
Meters	m
Metre per minute	m min^{-1}
Micro Metre	μm
Milimeters	mm
Nano metres	nm
Newtons	N
Numerical Control	NC

Oxygen	O₂
Silicon Nitride	Si₃N₄
Theta	θ
Two times the average flaw size (2c)	a
Young's Modulus	E
Zirconia Oxide	ZrO₂

Figures

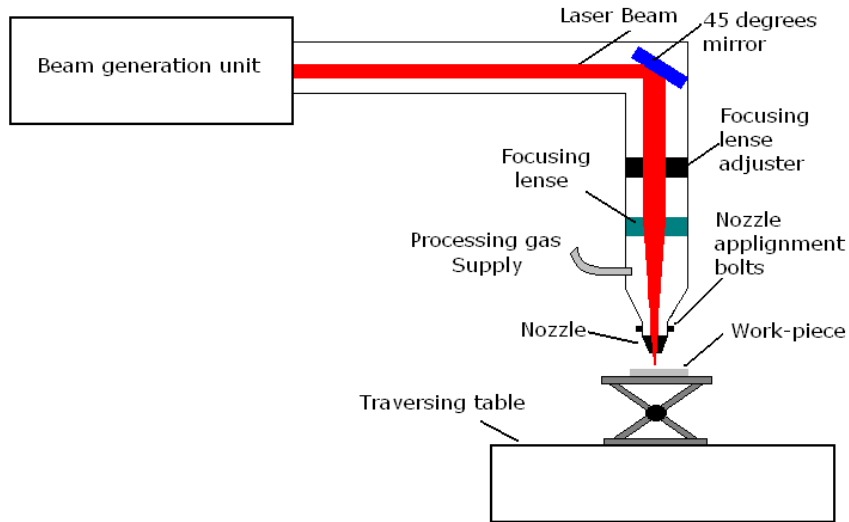


Figure 1 Schematic diagram showing the experimental set-up of the CO₂ laser surface treatment of the ZrO₂ and the Si₃N₄ engineering ceramics.

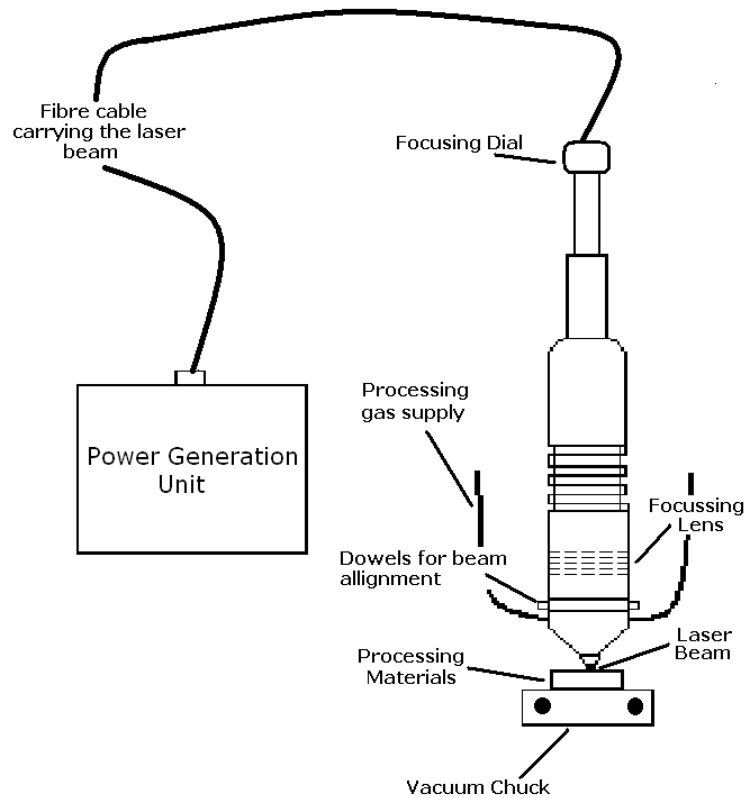


Figure 2 Schematic diagram showing the experimental set-up of the fibre laser surface treatment of the ZrO₂ and the Si₃N₄ engineering ceramics.

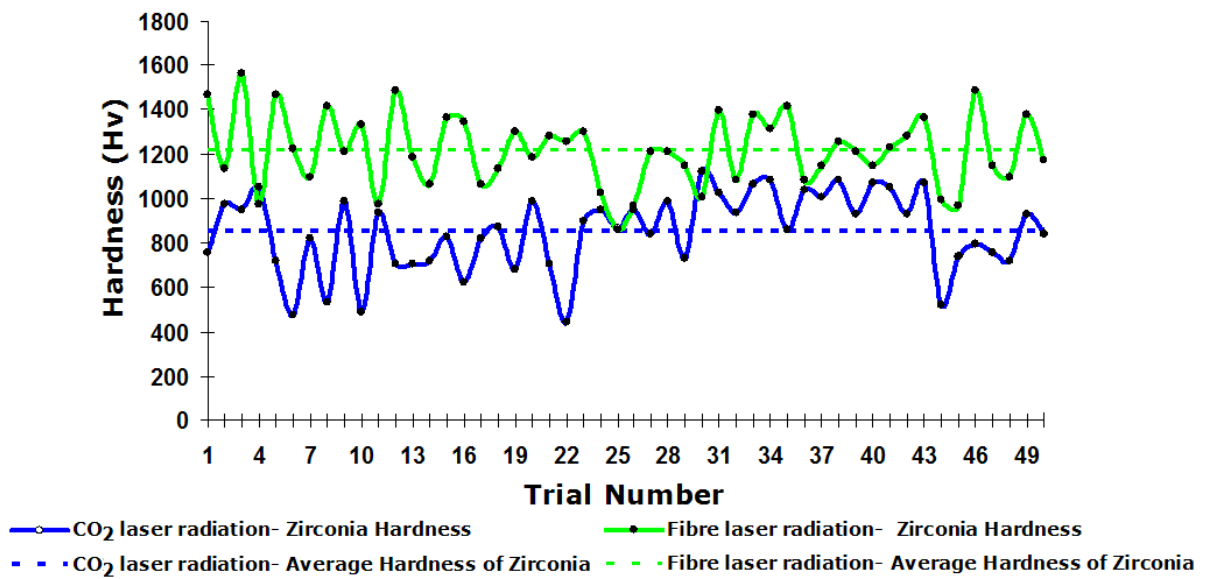


Figure 3 Hardness of the ZrO₂ ceramic treated with a CO₂ and a fibre laser radiation.

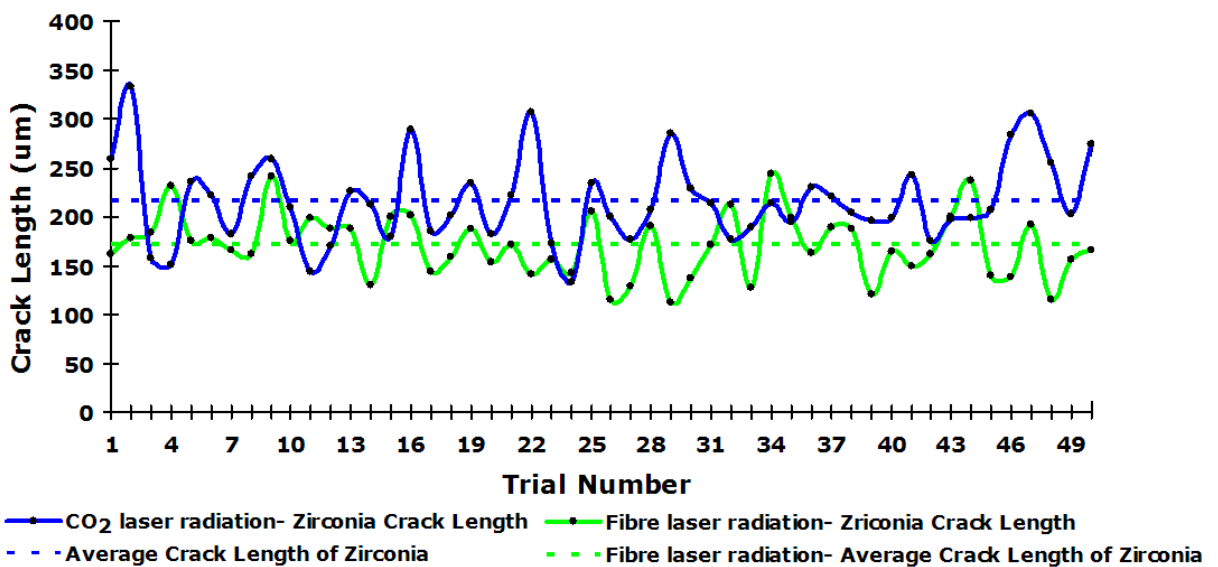


Figure 4 Crack length of the ZrO₂ ceramic obtained after a CO₂ and a fibre laser radiation.

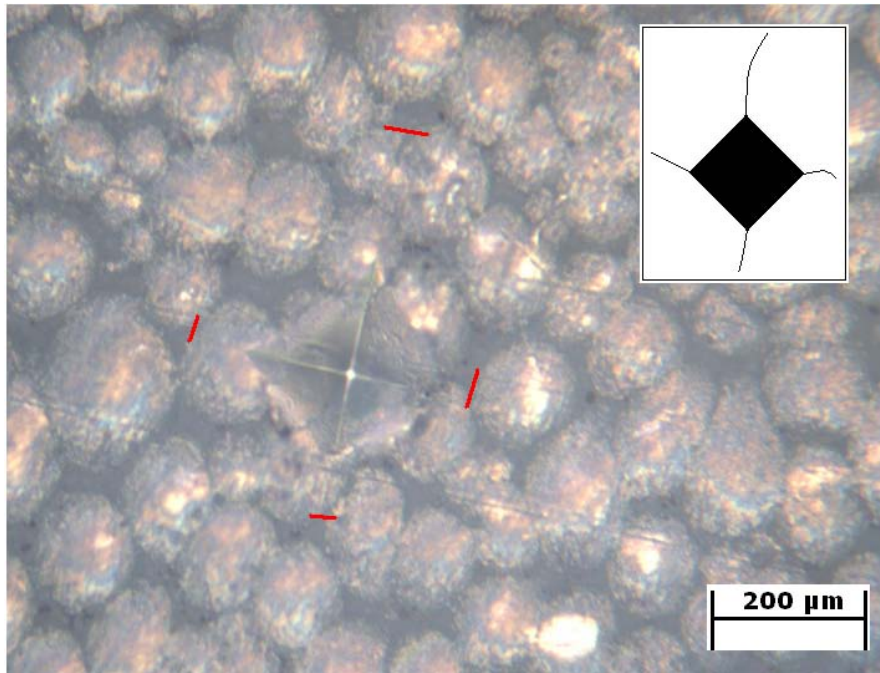


Figure 5 Optical image of the CO₂ laser radiated surface of the ZrO₂ ceramic indented by a 49.05 N load; 600 mm/min; 3 mm post size; (hardness = 650 (Hv); crack length = 298 μm; $K_{IC} = 2.75 \text{ MPa m}^{1/2}$).

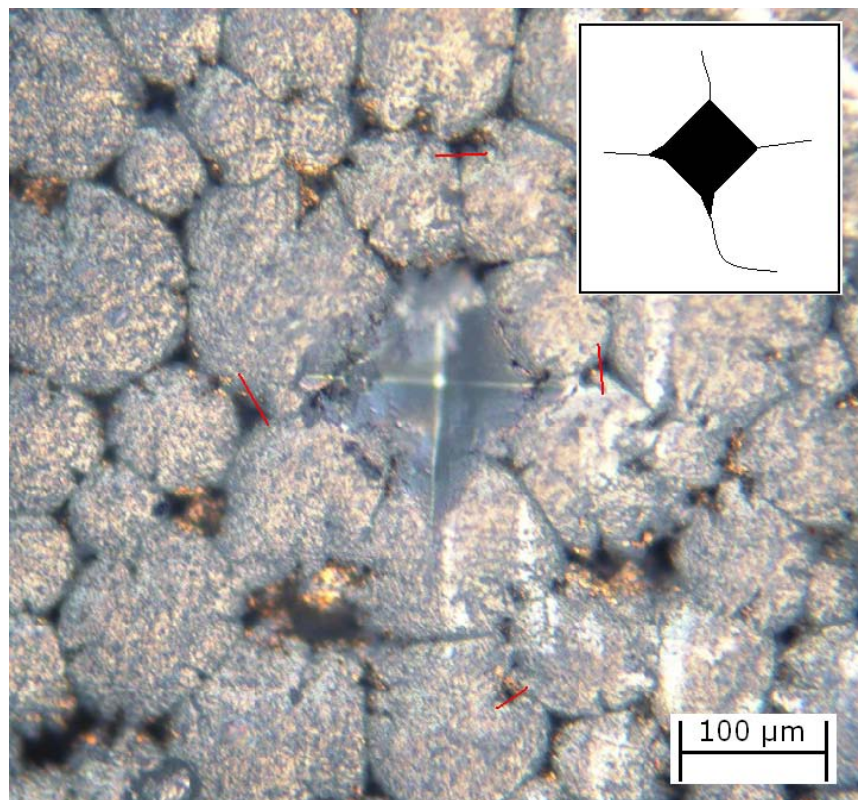


Figure 6 Optical image of the fibre laser radiated surface of the ZrO₂ ceramic indented by a 49.05 N load, 600 mm/min, 3 mm post size, hardness = 654 (Hv), crack length = 232 μm, K_{1c} = 3.97 MPa m^{1/2}).

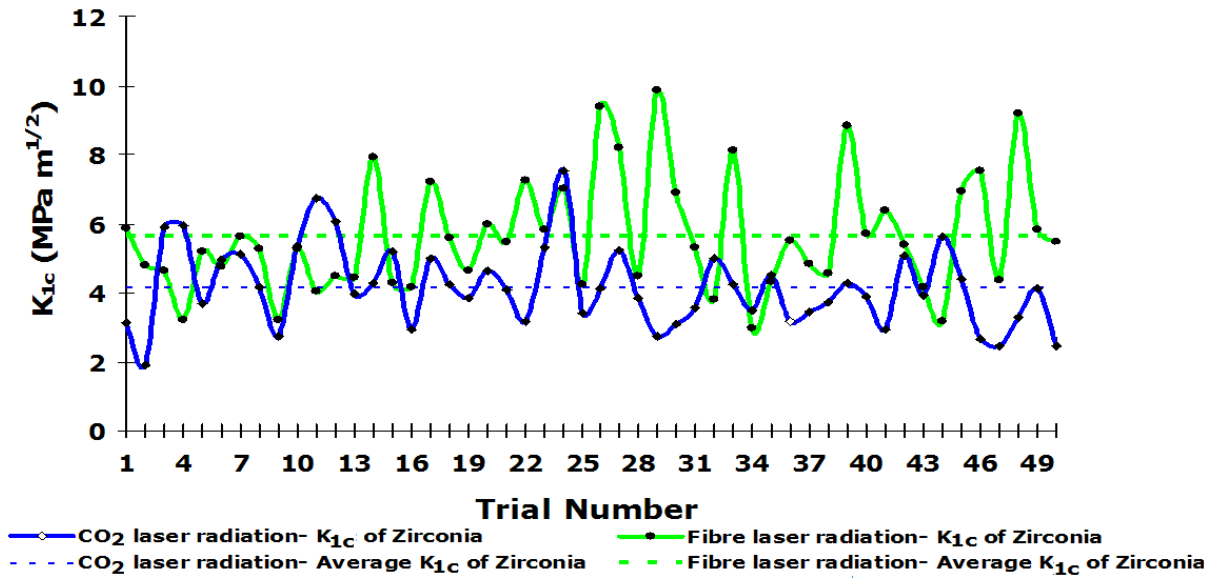


Figure 7 K_{1c} of the ZrO₂ ceramic obtained after the CO₂ and a fibre laser radiation.

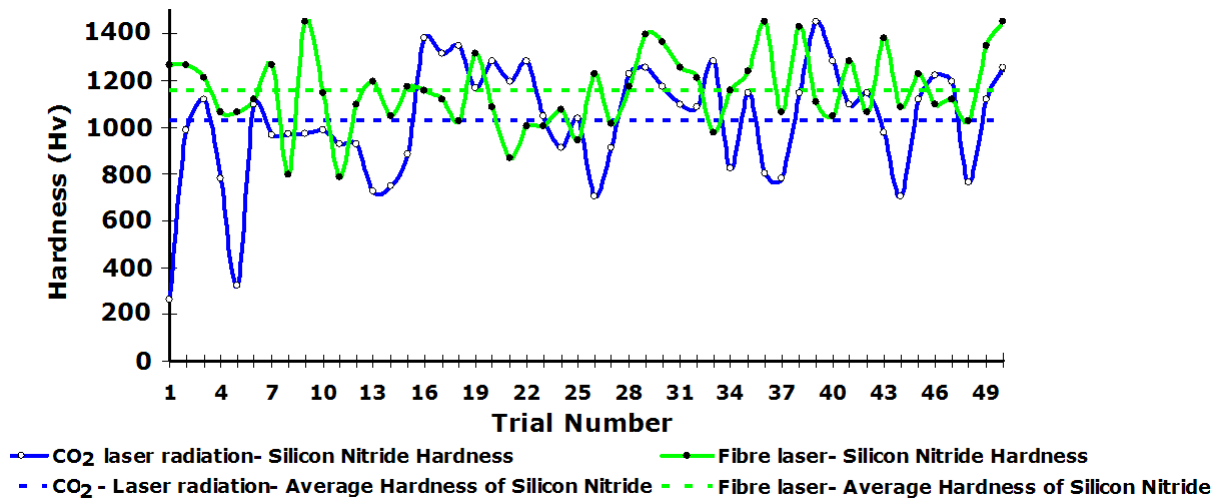


Figure 8 Hardness of the Si₃N₄ ceramic treated by CO₂ and a fibre laser radiation.

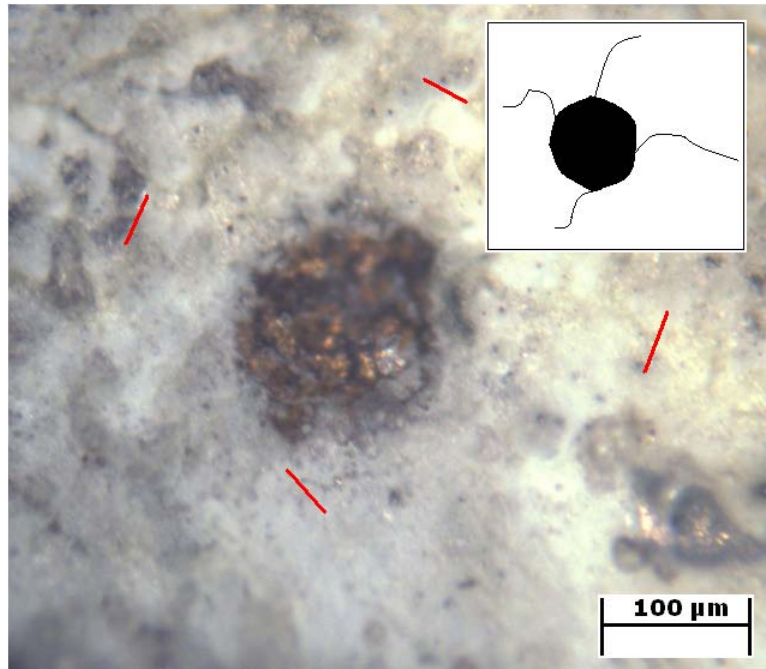


Figure 9 Optical image of the CO₂ laser treated surface of Si₃N₄ ceramic indented by a 49.05 N load, laser power = 150 W; 100 mm/min; 3 mm post size; (hardness = 623 Hv); crack length = 281 μm, K_{1C} = 3.58 MPa m^{1/2}).

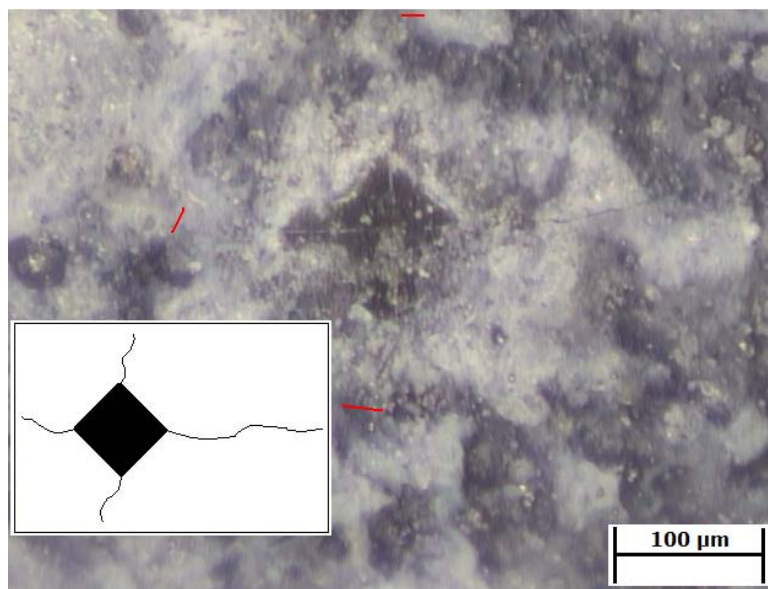


Figure 10 Optical image of the fibre laser treated surface of Si₃N₄ ceramic indented by a 49.05 N load; laser power = 150 W; 100 mm/min; 3 mm post size; (hardness = 900 Hv; crack length = 248 μm; K_{1C} = 3.59 MPa m^{1/2}).

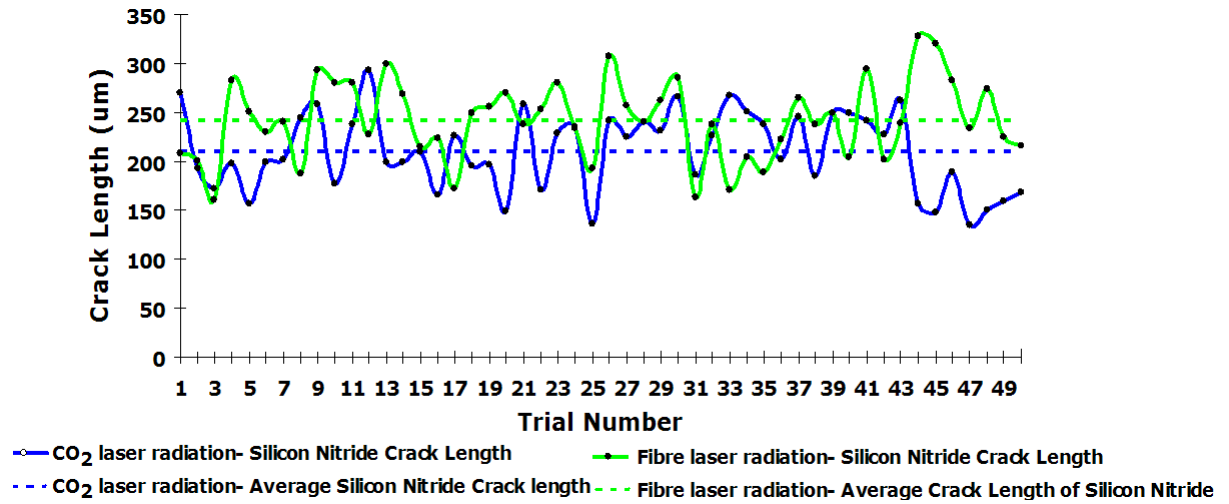


Figure 11 Crack length of the Si₃N₄ ceramic obtained after a CO₂ and a fibre laser radiation.

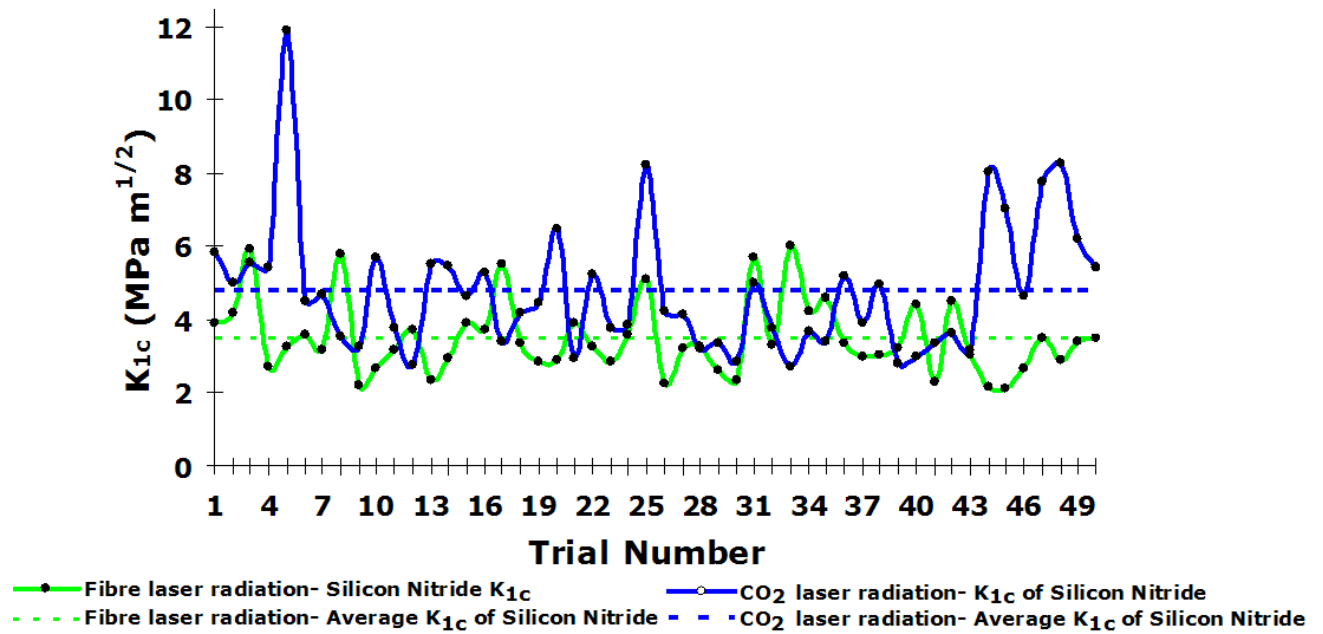


Figure12 K_{1c} of the CO₂ laser treated surface of the Si₃N₄ ceramic.

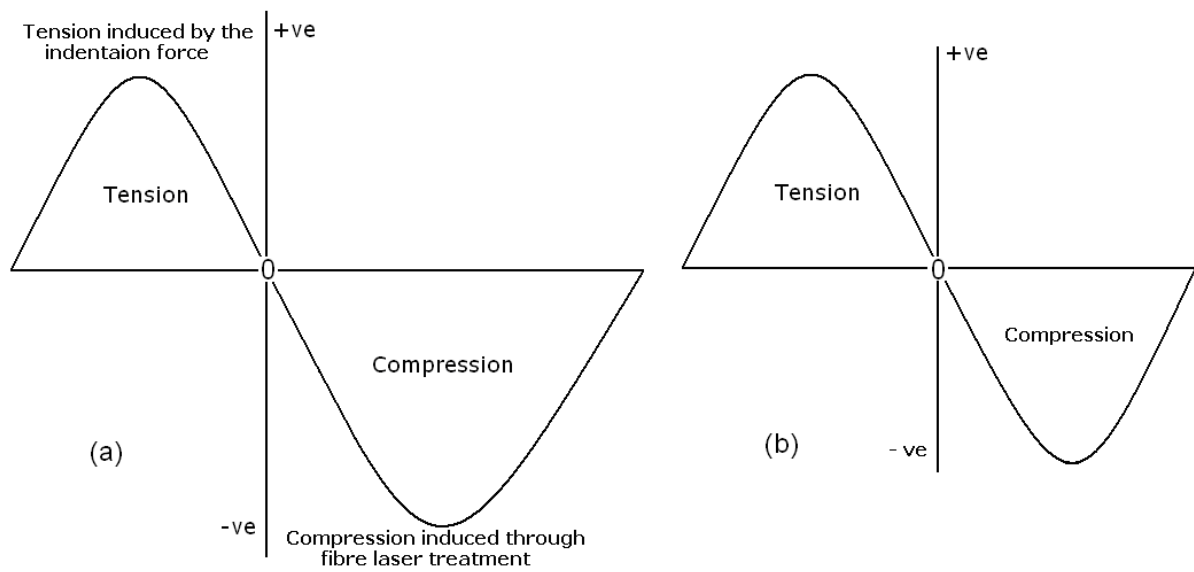


Figure 13 Schematic representation of tension and compression concept where (a) the increase in induced compression from the fibre laser surface treatment and (b) showing state of the ceramic under equilibrium condition.

Tables

Table 1 Surface hardness, crack lengths and the K_{IC} values found by using 5 kg indentation load from the experimental investigation of both the Si_3N_4 and the ZrO_2 engineering ceramics treated by the CO_2 and the fibre laser radiation.

	Average Surface hardness (Hv)						Average surface crack length (μm)						Average surface K_{IC} ($MPa m^{1/2}$)					
	Si_3N_4	STVD	Range	ZrO_2	STVD	Range	Si_3N_4	STVD	Range	ZrO_2	STVD	Range	Si_3N_4	STVD	Range	ZrO_2	STVD	Range
As-received surface	1106	201	707 - 1648	983	141.37 17	707- 1330	386	0.0008 65	227 - 499	278	0.0007 07	178 - 512	1.71	0.59	0.55 - 3.06	2.45	0.83	0.92 - 4.42
CO_2 laser treatment	1019	216	666 - 1379	854	178	473 - 1120	278	0.0006 09	179 - 463	216	0.0004 34	144 - 333	3.16	1.17	1.13 - 5.30	3.75	1.05	1.69 - 6.78
Fibre laser treatment	1154	159	788 - 1449	940	60	826 - 1089	242	0.0004 07	160 - 307	170	0.0003 28	112 - 243	3.25	0.94	1.95 - 5.52	5.05	1.51	2.67 - 8.86